Supplemental material for:

Title: Spectral integration in primary auditory cortex due to temporally precise convergence of thalamocortical and intracortical input

Abbreviated title: Temporally precise spectral integration in auditory cortex

Authors: Max F.K. Happel[1,2,*], Marcus Jeschke[1,*] and Frank W. Ohl[1,2]

Contents:

(1) Temporal features of current flow (AVREC waveform) reflect afferent bottom-up and intracortical contributions

The averaged rectified CSD (AVREC) can be used to examine the temporal features of overall current flow in tissue sampled during one penetration of a multielectrode (cf. Givre et al., 1994, Schroeder et al., 1998). Because of the loss of information about the direction of current flow (due to rectification) the AVREC itself does not provide information that helps dissociating contributions from afferent or intracortical generators of the current flow (Givre et al., 1994). In the present study we relate the CSD profile to the resultant AVREC waveform before and after cortical silencing (Suppl. Fig.1). The AVREC of primary auditory cortex in gerbil showed a multi-phasic waveform similar to previous studies in primates (Givre et al., 1994, Schroeder et al., 1998).

The intial phase (1) showed the highest amplitude and overlapped with a second phase (2). The subsequent longer-latency phase (3) was clearly separated and smaller in amplitude (Suppl.Fig.1*A*). Phases (1) and (2) were temporally related to strong granular activations (see CSD) and phase (3) was related clearly to phases of extragranular activations. Cortical silencing abolished phases (2) and (3) which is indicative of their predominantly intracortical origin (Suppl.Fig.1*B*). Furthermore, the initial phase (1) showed a decrease in peak amplitude after drug application of about 10-fold (peak amplitude before: 1.48 mV/mm^2 and after: 0.14 V/mm^2 cortical silencing), which is in good correspondence to the observed mean peak amplitude reduction of the granular sink S1 (see main article and Tab.1). We also compared the integral of the AVREC before and after drug application for a 200 ms window and found cortical silencing to reduce the cortical net activation between 40-85%, depending on stimulation frequency (data not shown). This is in good correspondence to the data on thalamocortical-recipient cells reported by Liu et al. (2007). These authors found the mean tone-evoked excitatory synaptic input to be reduced about 39%. We found reduction in AVREC amplitude after BF stimulation also within the short time window, in which no significant relative residuals were found (see red bars in Suppl. Fig.1 at +8 ms after AVREC onset, cf. Fig. 7A). Hence, intracortical amplification of afferent input via recurrent excitations do not significantly contribute to the relative residual of the CSD (for further discussion see main text). We therefore conclude that pharmacological silencing of the intracortical

microcircuitry blocks the activation of intracolumnar synaptic populations associated with recurrent microcircuits and additional intercolumnar synaptic contributions as well.

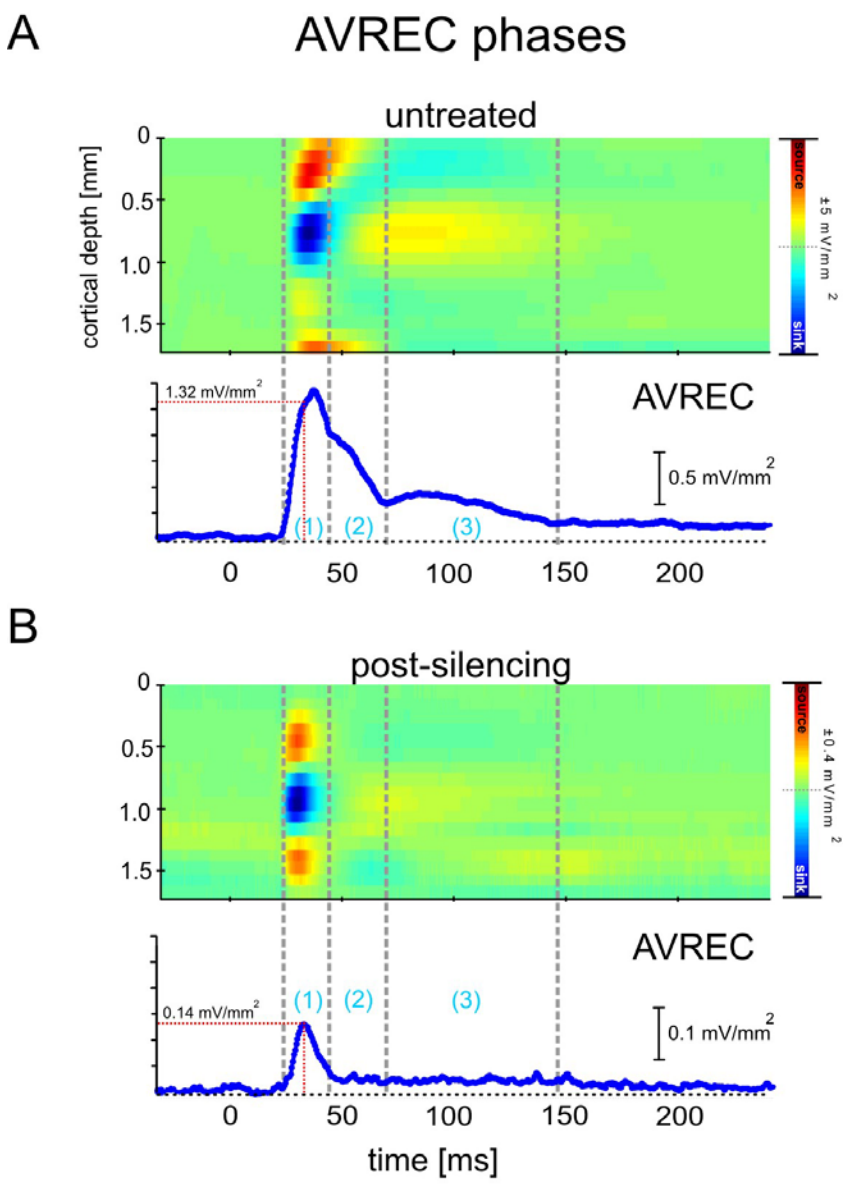

Suppl. Figure 1. ***A***, Representative example of a multi-phasic AVREC waveform in primary auditory cortex (stimulation with BF) extending temporally up to 125 ms post stimulus onset, including phase (3). ***B***, After cortical silencing, the initial phase (1) showed a 10-fold decrease of peak amplitude. Phases (2) and (3) were blocked completely after drug application. Furthermore, the red bar in both plots indicates onset latency of the relative residual of the CSD. Respective AVREC amplitudes are indicated.

(2) Immunohistochemistry and histology

Animals were killed by intracardial injection of 0.5 ml T61 (Intervet) following the acute experiments. Brains were removed and cut as described in the main paper (n=5). Suppl.Fig. 2 demonstrates the perpendicular insertion of the electrode as indicated by the depleted area of cell bodies (Nissl staining). Positioning of channel 1 of the electrode array always at the cortical surface allowed us to relate all electrodes to the cortical depth of recording. Cortical layers display interindividual differences. Therefore, cortical layers have been identified on the basis of Nissl stains according to previous anatomical studies (Budinger et al., 2000b). Suppl. Table 1 shows interindividual differences of cortical layers for 5 animals. Typical data shown in the main manuscript were taken from animal 1 (cf. Figs.1 and 2).

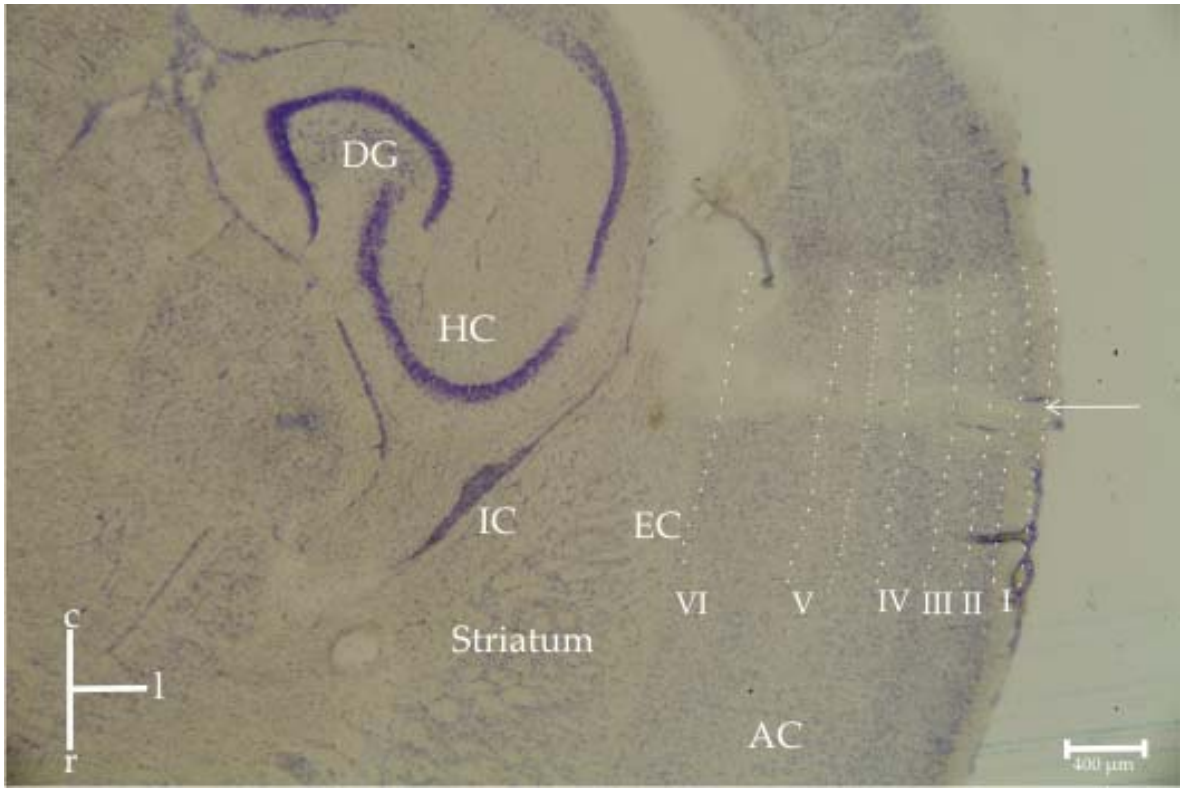

Suppl. Figure 2. Representative example of histological analysis illustrating how measured CSD profiles were referred to cortical depths and corresponding cortical layers. The white arrow marks the insertion canal of the multielectrode perpendicular to the cortical surface. Cortical layers have been identified on the basis of Nissl stains according to previous anatomical studies (Budinger et al., 2000b). HC – hippocampus. DG – dentate gyrus of HC. EC – capsula externa. intracortical – capsula interna. AC – auditory cortex. I-VI – cortical layers. Arrow indicates insertion point of shaft electrode. Bar indicates 400 µm.

Suppl.Table 1. Interindividual differences of the relation between cortical layers and laminar depths.

Animal	Cortex (AI) and layer-thickness [µm]							Sink S1 [µm]
	Cortex	Layer I	II	III	IV	V	VI	post-silencing
1	1697	144	154	156	388	612	243	375
2	1560	69	106	107	151	547	622	195
3	1618	127	227	289	166	300	488	180
4	1714	135	246	381	168	244	531	180
5	1593	91	127	161	209	485	520	160
MW±SEM	1636±29.8	113.2±14.2	172±27.6	218.8±50.5	216±44	437.6±71.1	480.8±63.5	238±37.3

Comparative histological borders revealed interindividual differences of cortical layer thickness. We therefore referred mainly to cortical depth in the quantitative analysis of CSD profiles. The typical example that we showed in the main manuscript (Fig. 1 and 2) was shown with individually determined cortical layers (animal 1). Nevertheless, we found the described sink components to be related to cortical layers in every animal. (One-way Pearson rank correlation coefficient between thickness of layer 4 and spatial extent of sink S1 after silencing: R = 0.972, p=0.003). Robust activations were found mainly in layer IV or border to layer IIIb, sometimes extending to upper layer Va (please note slightly higher mean values for extension of granular sink S1, compared to thickness of layer IV). Activations in cortical depths corresponding to layer I-IIIa were blocked by cortical silencing in all cases. We therefore discussed sink components with relation to cortical layers and the known intracortical microcircuitry. In Fig. 4 we indicated cortical layer relations as revealed in the mean population data (n=5).

(3) Hypothesized framework for cortical spectral integration

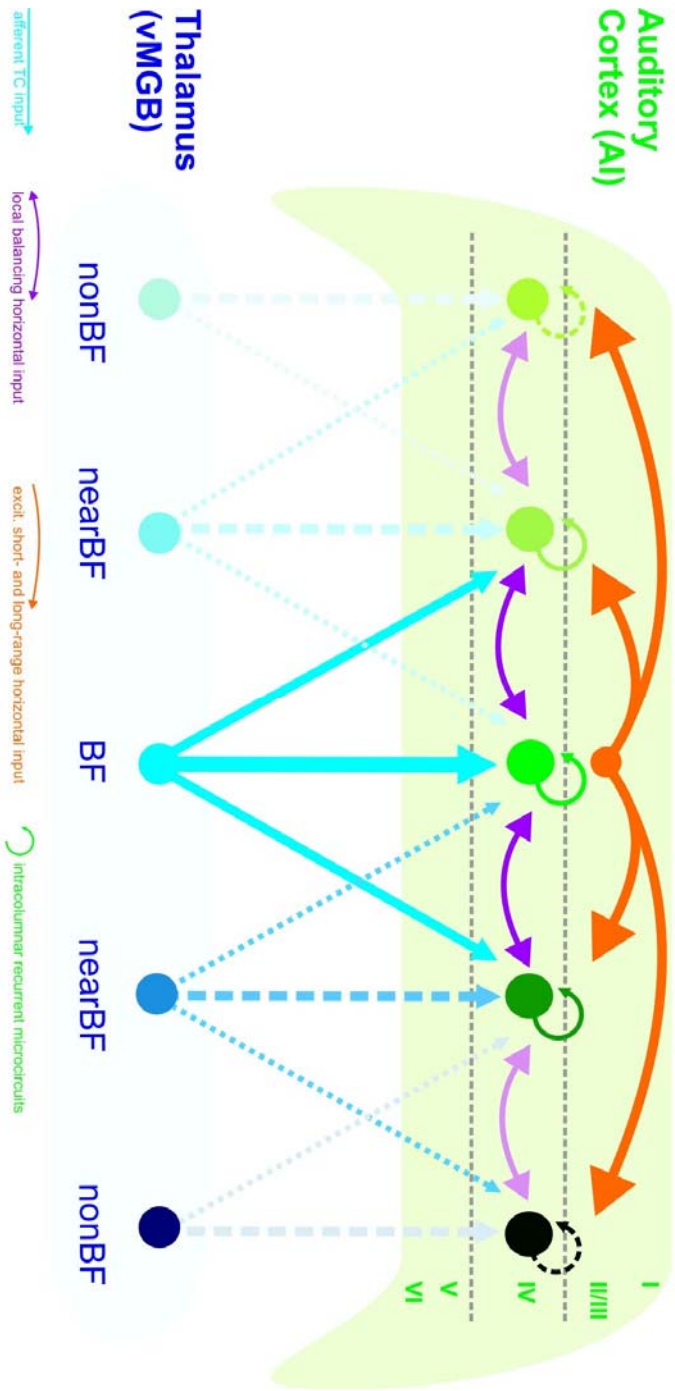

Suppl. Figure 3. Proposed framework of convergent thalamocortical and local and global intracortical inputs. Afferent input is integrated with intracolumnar (recurrent) and horizontal (intercolumnar) short- and long-range intracortical inputs stemming from broad parts of the primary auditory cortex.